Journal of Alloys and Compounds 657 (2016) 889–892

Contents lists available at ScienceDirect

Journal of Alloys and Compounds

journal homepage: http://www.elsevier.com/locate/jalcom

Yield strength of Ni–Al–Cr superalloy under pressure

S.V. Raju [a, *], B.K. Godwal [b], J. Yan [c, d], R. Jeanloz [b, e], S.K. Saxena [a]

[a] CeSMEC, Dept. of Mechanical Engg., Florida International University, Miami, FL 33172, USA
[b] Earth and Planetary Science, University of California, Berkeley, USA
[c] Advanced Light Source, Lawrence Berkeley National Laboratory, Berkeley, CA 94730, USA
[d] Earth & Planetary Science Department, University of California, Santa Cruz, CA 95064, USA
[e] Miller Institute for Basic Research in Science and Department of Astronomy, University of California Berkeley, CA 94720, USA

ARTICLE INFO

Article history:
Received 27 August 2015
Received in revised form
7 October 2015
Accepted 12 October 2015
Available online 23 October 2015

Keywords:
Metals and alloys
Rapid-solidification
Quenching
Elasticity
Mechanical properties
Strain
High pressure
X-ray diffraction

ABSTRACT

Ni based superalloy Ni–Al–Cr with γ and γ′ phase was studied under high pressure up to 30 GPa using diamond anvil cell technique. In-situ X-ray diffraction data was collected on these alloys under hydrostatic and non-hydrostatic conditions. Cubic phase remains stable up to the highest pressure of about 30 GPa. Bulk modulus and its pressure derivative obtained from the volume compression of pressure data are K = 166.6 ± 5.8 GPa with K′ set to 4 under hydrostatic conditions and K = 211.3 ± 4.7 GPa with K′ set to 4 for non-hydrostatic conditions. Using lattice strain theory, maximum shear stress 't' was determined from the difference between the axial and radial stress components in the sample. The magnitude of shear stress suggests that the lower limit of compressive strength increases with pressure and shows maximum yield strength of 1.8 ± 0.3 GPa at 20 GPa. Further, we have also determined yield strength using pressure gradient method. In both the methods, yield strength increases linearly with applied pressure. The results are found to be in good agreement with each other and the literature values at ambient conditions.

1. Introduction

Ni–Al based alloys are widely being used as high strength superalloys in aerospace engineering and high temperature industrial applications. In the Ni–Al phase diagram [1], Ni_3Al with $L1_2$ type structure has the highest strength among the Ni–Al systems [2,3]. Addition of 'Cr' to Ni_3Al superalloy stabilizes the γ and γ′ region of the crystal structure and is also known to improve ductility and corrosive properties [4,1]. The elastic properties of Ni_3Al with $L1_2$ structure has been studied both experimentally and using first principles density functional theory (DFT) for bulk modulus, shear modulus and elastic anisotropy [5]. Shulson et al., 1985 [6] established a relationship between effect of grain size (d = 2.9–1100 μm) on the yield strength of Ni_3Al at room temperature. Further, he reported yield strength of stoichiometric and non-stoichiometric Ni–Al alloys within the context of the structure and chemistry at the grain boundaries and discussed it in terms of the transmission of slip through either an ordered or a constitutionally disordered grain boundary [7]. Recent studies on the elastic properties of Ni–Al alloyed with Cr(7.5 at%) using in-situ X-ray diffraction under high pressure, and using nano-indentation techniques suggest that micro alloying with Cr although decreases the strength improves ductility and corrosive properties [8]. From the literature, Cr is known to preferentially partition to the γ phase of Ni_3Al as the atomic radius of Cr is very similar to that of Ni [8,9]. Geng et al., 2005 [10] calculated shock Hugoniot of Ni_3Al in $L1_2$ structure with an equation of state (EOS) based on a cluster expansion and variational methods and reported an order-disorder transition occurring at shock pressure of 205 GPa with temperature of 3750 K.

Yield strength is an important indicator for the most engineering designs, which is influenced by several factors such as raw material quality, chemical composition, forming process, heat treatment process, etc. Yielding of a material is typically measured using load versus displacement method at 1 atm. Knowledge of stress variation in materials on application of pressure or temperature is of fundamental importance to extract as well as model thermodynamic and elastic properties of the material [11–15]. Diamond anvil cell techniques are well established for the study of

* Corresponding author.
E-mail address: sraju@fiu.edu (S.V. Raju).

http://dx.doi.org/10.1016/j.jallcom.2015.10.092
0925-8388/

elastic properties and phase transitions. Using elastic strain theory [16,17], it is shown that yield strength of the solids can be determined quantitatively from in-situ methods such as pressure gradient method [12], the X-ray diffraction peak broadening analysis [18,19] and the radial X-ray diffraction peak shifts [20–22]. In addition, in-situ X-ray diffraction method using diamond anvil cell allows us to measure shear strength in solids with applied load. Here, we present the yield strength measurements of Ni–Al–Cr determined by two different methods: in-situ X-ray diffraction and pressure gradient measurements.

2. Experimental

Ni_3Al alloyed with Cr (7.5 at %) was prepared by arc melting and directional solidification methods. Stoichiometric compositions of elemental powders were made into a pellet and arc melted under vacuum [23]. The samples were annealed at 1473 K under vacuum for seven days to further reduce the internal strain developed during melt and quenching. Presence of γ and γ′ phases were confirmed from images obtained using High-annular angle dark field (HAADF) technique. Further, electron diffraction spectroscopy (EDS) maps confirmed the ratio of alloying material, the details of which can be found elsewhere [8]. Diffraction patterns were found to be consistent with cubic Pm-3m(γ′) and Fm3m(γ) structures. Lebail fitting using GSAS [24] resulted in a = 3.567 ± 0.005 Å and v = 45.38 ± 0.05 $Å^3$ in agreement with literature values [25,26].

In-situ X-ray diffraction studies were carried out on Ni–Al–Cr using diamond anvil cell at beamline 12.2.2, of Advanced Light Source (ALS), LBNL employing angle dispersive geometry using wavelength of 0.4959 Å. Two separate experiments were carried out; In the first one, sample was loaded with Methanol + ethanol in the ratio 4:1 which served as the pressure transmitting medium. The details of the experimental set-up can be found elsewhere [27]. For non-hydrostatic measurements, fine grains of Ni–Al–Cr alloy along with few specks of NaCl were loaded in diamond anvil cell. The sample was loaded in a stainless steel gasket which was pre-indented to 50 μm thickness and drilled with a 200 μm hole. A ruby chip few microns thick loaded along with sample was used for pressure measurement. Prior to this experiment, we had attempted to study the equation of state of Ni–Al–Cr at beamline 16IDB of HPCAT, Advanced Photon Source, Chicago. We found the P–V data obtained from the measurements were largely scattered. Later, we found this was due to large pressure gradients caused by the sample itself as it was superhard material chunks. We did not powder them due to the possibility that the ordering might be lost during the process. It created a large discrepancy between the pressure measured from platinum which was used as the x-ray standard and the measured P–V data of the alloy. Hence, we repeated the experiments at BL12.2.2, Advanced Light Source on fine grains of Ni–Al–Cr with few specks of NaCl as pressure marker.

Evolution of diffraction pattern as a function of pressure for Ni–Al–Cr under hydrostatic conditions is shown in Fig. 1(a) and (b). Crystal structure of Ni–Al–Cr is found to be stable up to 30 GPa, the highest pressure studied.

3. Results and discussion

Yield strength from equation of state:

Pressure-Volume data of Ni_3Al alloyed with Cr (7.5 at%) obtained from the X-ray diffraction data collected under hydrostatic and non-hydrostatic conditions were fitted using third order Birch–Murnaghan equation [29,30] of state,

$$P(V) = \frac{3B_0}{2}\left[\left(\frac{V_0}{V}\right)^{\frac{7}{3}} - \left(\frac{V_0}{V}\right)^{\frac{5}{3}}\right]\left\{1 + \frac{3}{4}(B_0'-4)\left[\left(\frac{V_0}{V}\right)^{\frac{2}{3}} - 1\right]\right\}. \quad (1)$$

From the fit, bulk modulus and its pressure derivative were determined. Bulk modulus K = 166.6 ± 5.8 GPa obtained under hydrostatic conditions and K = 211.3 ± 4 GPa was found under non-hydrostatic conditions with K′ set as 4.

Yield Strength (YS) is given by YS = $(\sigma_1 - \sigma_3)/2$ where σ_1 and σ_3 are maximum and minimum normal stresses in axial and radial directions. According to lattice strain theory, X-ray diffraction measures strains in radial direction as the offset between hydrostatic and non hydrostatic pressures at same volume, and is given by $2\tau/3$ with τ as the shear stress $(\sigma_1 - \sigma_3)$. We have measured the shear stress of Ni–Al–Cr from the pressure offset measured between hydrostatic and non-hydrostatic conditions at a constant volume which is shown in Fig. 2. Shear stress is found to increase linearly with applied axial load with a maximum shear stress of 1.8 GPa measured at applied load of 20 GPa.

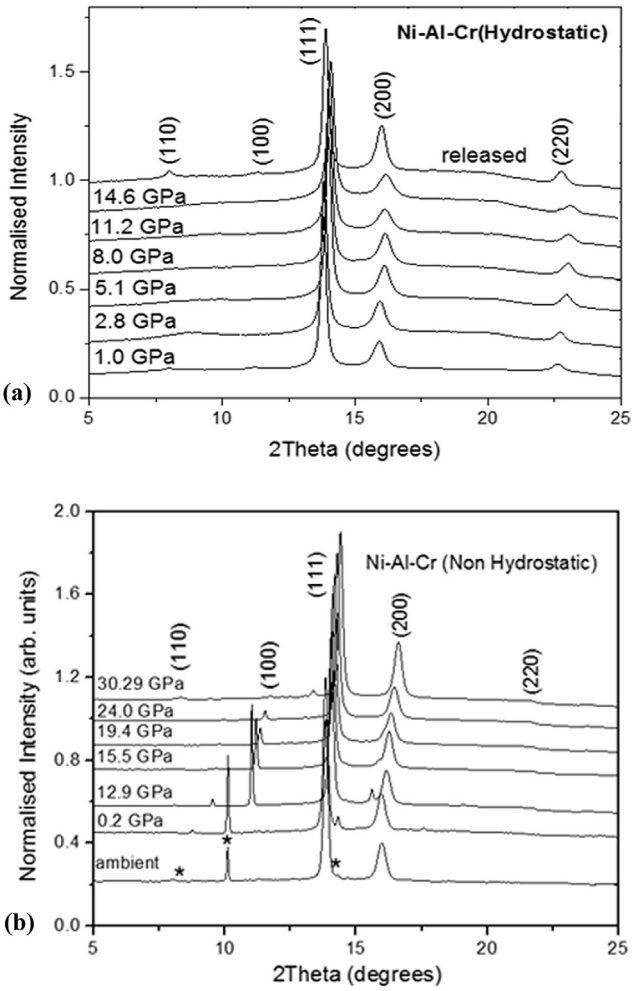

Fig. 1. (a): X-ray diffraction data of Ni–Al–Cr collected at WL 0.4959A at various pressures under hydrostatic conditions. (b). X-ray diffraction pattern of Ni–Al–Cr (7.5 at %) at various pressures under non-hydrostatic conditions with wavelength of 0.4959A. Asterisk sign represents line positions of NaCl which is used to determine pressure at each step from its equation of state [28]. Ni–Al–Cr peak (220) is weak due to preferred orientation.

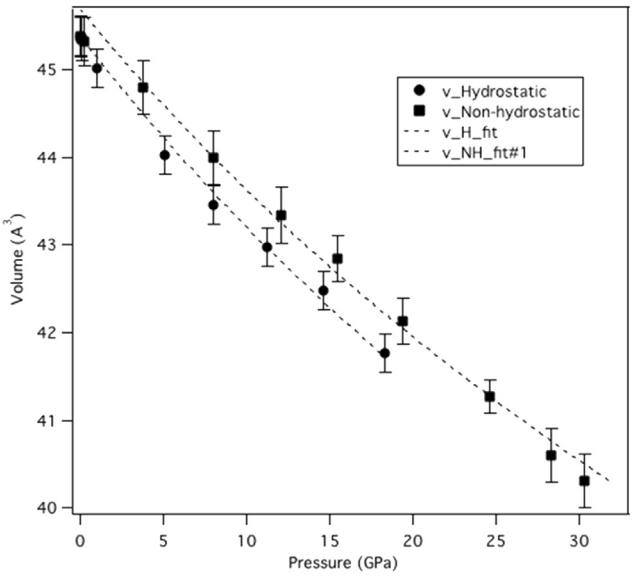

Fig. 2. Pressure vs. volume data obtained for Ni–Al–Cr under non-hydrostatic conditions is represented by solid squares. Hydrostatic data was obtained from our previous work [8] Broken lines represent their corresponding fits obtained using Birch–Murnaghan equation of state.

Yield strength by pressure gradient method: *Jeanloz* and coworkers [11,12,31] have obtained quantitative measure of shear stresses from the maximum (σ_1) and minimum (σ_3) normal stresses and related them to the pressure gradients($\delta P/\delta r$) across the sample; $\tau = (h/2)\,(\delta P/\delta r)$ with h as the sample thickness and r the radial distance perpendicular to the pressure axis. Pressure was measured across the Ni–Al–Cr sample loaded in diamond anvil cell under non-hydrostatic conditions. For this experiment, fine grains of Ni–Al–Cr alloy were loaded in a stainless steel sample chamber with 200 μm diameter hole and 50 μm thickness. Several ruby crystals of <5 μm grain size were evenly distributed across the entire sample chamber. Pressure was measured by fitting the ruby

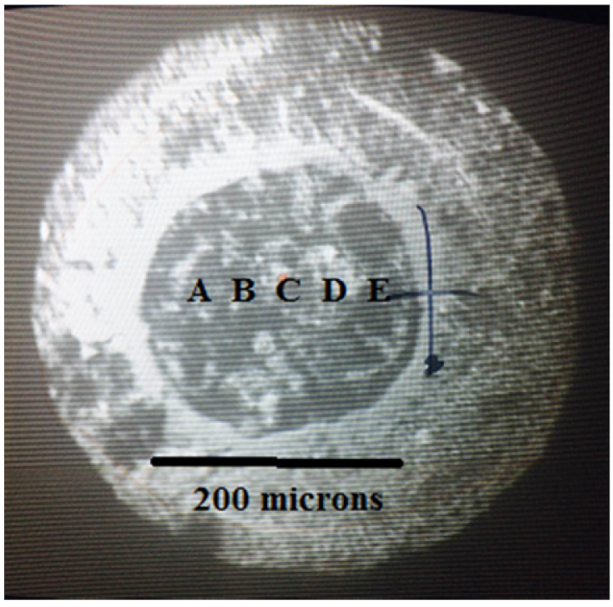

Fig. 3. Image of Ni–Al–Cr loaded in diamond anvil cell. Various positions at which the pressure was measured using ruby is indicated from A to E with increment of 30 μm apart.

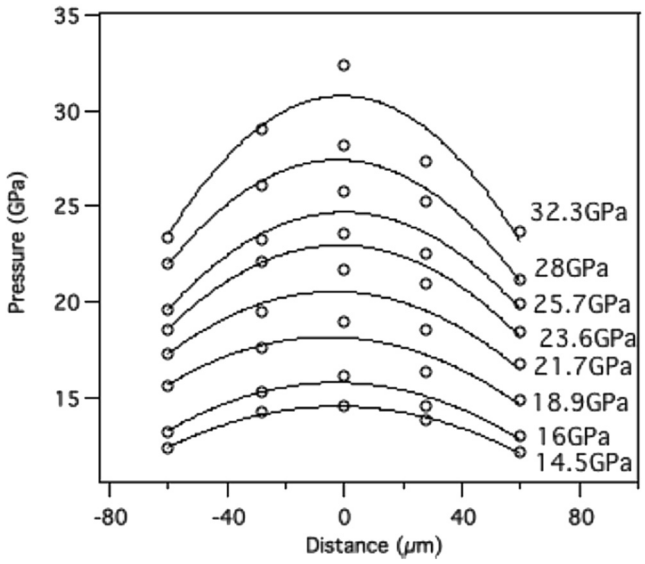

Fig. 4. Mean stress distribution across the Ni–Al–Cr alloy under non-hydrostatic conditions. Pressure at each radial position across the sample relative to the center of the sample chamber is indicated by each individual point as determined using ruby fluorescence method on the diamond sample interface. Each curve was obtained at the average sample pressure indicated.

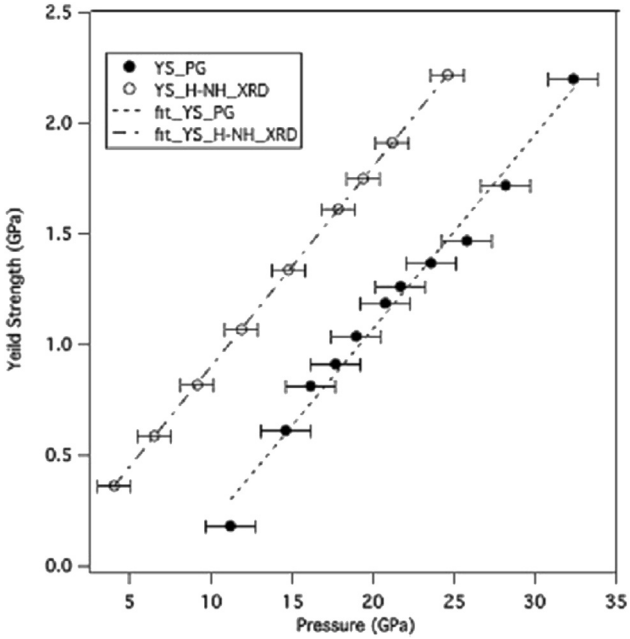

Fig. 5. Comparison of yield strength versus applied load. Solid circles represent data obtained from hydrostatic and non-hydrostatic equations of state (P–V relations) and open circles are obtained using pressure gradient method.

florescence measured as a function of distance of the sample from the center of the sample chamber. Pressure is determined from the non-hydrostatic pressure scale [32].

$$P = 380.8\left[(\Delta|\lambda/\lambda + 1)^5 - 1\right],$$

where, λ_0 is 694.2 nm, λ is redshift in nanometers, and P is pressure in gigapascals. Fig. 3, shows various positions at which the pressure was measured using ruby grains spread on the surface of Ni–Al–Cr up to 32 GPa.

Pressure distribution across the axially loaded sample, measured under non-hydrostatic conditions is shown in Fig. 4. Assuming sample response to be isotropic, the hydrostatic ruby pressure is given by $(\sigma_1 + 2\sigma_3)/3$ which is also equal to mean normal stress. Then, shear stress of Ni–Al–Cr can be determined using the relation $t = 3/2(\sigma_1 - \sigma_3)$ where, σ_3 is the confining pressure and σ_1 is equal to the load stress. For pressure gradient method, Yield strength is given by YS = h/2 (dP/dr), with, h the sample thickness and dP/dr is the radial pressure gradient measured from the center of the sample chamber.

Yield strength obtained from the equation of states (P–V relations) under hydrostatic, non-hydrostatic conditions and pressure gradient methods as a function of pressure are shown in Fig. 5. We find that the yield strength obtained from both the methods show linear increase with pressure. Further, we have determined the yield stress at 20 GPa and at a constant volume as the offset between non hydrostatic and hydrostatic isotherms and obtained a value of about 1.8 ± 0.3 GPa in reasonable quantitative in agreement with that found from pressure gradient method 1.1 ± 0.3 GPa.

4. Conclusion

Yield strength of Ni–Al–Cr is determined for varying the load up to 30 GPa using in-situ X-ray diffraction measurements and to the pressures of 35 GPa from pressure gradient method with diamond anvil cell. Both the methods show linear response for variation of yield strength with increasing pressure. Bei et al. [33], measured yield strength of Ni_3Al using tensile measurements and found to be in the range of 400–600 MPa which is in close agreement with that obtained for Ni–Al–Cr using diamond anvil cell methods. The increase in yield strength under pressure could be due to the increase in number of defects and dislocations known to occur at high pressures. This is similar to the effect when the alloy is subjected to the mechanical treatment for severe plastic deformation (SPD) which is established method to improve the strength of the material. In general, using these methods one can expect a slope change on the yield strength plot when a material undergo phase transformation. Hence, further work on yield strength studies on an alloy with known phase transformation under pressure can provide insight to improve our understanding of deformation mechanisms.

Acknowledgments

The authors acknowledge support from the Air Force Office of Scientific Research (Grant No. FA9550-12-1-0456). The Advanced Light Source is supported by the Director, Office of Science, Office of Basic Energy Sciences, of the U.S. Department of Energy under Contract No. DE-AC02-05CH11231. Portions of this work were performed at HPCAT (Sector 16), Advanced Photon Source (APS), Argonne National Laboratory. HPCAT operations are supported by DOE-NNSA under Award No. DE-NA0001974 and DOE-BES under Award No. DE-FG02-99ER45775, with partial instrumentation funding by NSF. The Advanced Photon Source is a U.S. Department of Energy (DOE) Office of Science User Facility operated for the DOE Office of Science by Argonne National Laboratory under Contract No. DE-AC02-06CH11357.

References

[1] G.K. Dey, Sadhana 28 (2003) 247–262.
[2] A. Chiba, S. Hanada, J. Mater. Sci. Technol. 9 (1993) 391–399.
[3] C. Barrett, T.B. Massalski, The structure of metals and alloys, in: Structure of Metals, third ed., 1980, pp. 223–269 (New York: Pergamon) Chap. 10.
[4] S.W. Guan, W.W. Smeltzer, Oxid. Metals 42 (1994) 375–391.
[5] S. Boucetta, T. Chihi, B. Ghebouli, M. Fatmi, Mater. Sci. Pol. 28 (1) (2010).
[6] E.M. Schulson, T.P. Weihs, D.V. Viens, I. Baker, Acta Metall. 33 (9) (September 1985) 1587–1591.
[7] E.M. Schulson, Y. Xu, P.R. Munroe, S. Guha, I. Baker, Acta Metall. Mater. 39 (1991) 2971–2975.
[8] S.V. Raju, A.A. Oni, B.K. Godwal, J. Yan, V. Drozd, S. Srinivasan, J.M. LeBeau, K. Rajan, S.K. Saxena, J Alloys and Compounds 2014, J. Alloys Compd. 619 (2015) 616–620.
[9] Y. Wang, Z.-K. Liu, L.-Q. Chen, Acta Mater. 52 (2004) 2665–2671.
[10] H.Y. Geng, N.X. Chen, M.H.F. Sluiter, Shock induced order-disorder transformation in Ni_3Al, Phys. Rev. B 71 (1) (2005) 012105.
[11] R. Jeanloz, B.K. Godwal, C. Meade, Nature 349 (1991) 687–689.
[12] C. Maede, R. Jeanloz, J. Geophys. Res. 93 (1988) 3261–3269.
[13] C. Maede, R. Jeanloz, J. Geophys. Res. 93 (1988) 3270–3274.
[14] C. Maede, R. Jeanloz, Science 241 (1988) 1072–1074.
[15] C. Maede, R. Jeanloz, Phys Rev. B. 41 2532 (190).
[16] A.K. Singh, J. Appl. Phys. 73 (1993) 4278.
[17] A.K. Singh, C. Balasingh, J. Appl. Phys. 75 (1994) 4956.
[18] D.J. Weidner, Y. Wang, M.T. Vaughan, Geophys. Res. Lett. 21 (1994) 753.
[19] J. Zhang, L. Wang, D.J. Weidner, T. Uchida, J. Xu, Am. Mineral. 87 (2002) 1005.
[20] H.K. Mao, J. Shu, G. Shen, R.J. Hemley, B. Li, A.K. Singh, London, Nature 396 (1998) 741.
[21] T.S. Duffy, G. Shen, J. Shu, H.K. Mao, R.J. Helmley, A.K. Singh, J. Appl. Phys. 86 (1999) 6729.
[22] D. He, T.S. Duffy, Phys. Rev. B 73 (2006) 134106.
[23] Larry Jones, BES Interlaboratory Study of Ni_3Al, Pittsburgh Airport Marriott Hotel, December 15–16, 1987.
[24] A.C. Larson, R.B. Von Dreele, "General Structure Analysis System (GSAS)", Los Alamos National Laboratory Report LAUR 86-748, 1994.
[25] M. Hansen, Constitution of Binary Alloys, McGraw-Hill, New York, 1958, p. 119.
[26] R. Ramesh, B. Pathiraj, B.H. Kolster, J. Mater. Sci. 29 (1994) 4764–4770.
[27] M. Kunz, A.A. MacDowell, W.A. Caldwell, D. Cambie, R.S. Celestre, E.E. Domning, R.M. Duarte, A.E. Gleason, J.M. Glossinger, N. Kelez, D.W. Plate, T. Yu, J.M. Zaug, H.A. Padmore, R. Jeanloz, A.P. Alivisatos, S.M. Clark, J. Synchrotron Radiat. 12 (2005) 650;
[27a] . APS HPCAT 16-IDB.
[28] F. Birch, J. Geophys. Res. 91 (B5) (1986) 4949.
[29] F. Birch, Phys. Rev. 71 (1947) 809.
[30] F.D. Murnaghan, Proc. Nat. Acad. Sci. 30 (1944) 244.
[31] C.M. Sung, C. Goetze, H.K. Mao, Rev. Sci. Instrum. 48 (1977) 1386.
[32] J. Xu, H.K. Mao, P.M. Bell, Acta Phys. Sin. 36 (1987) 500.
[33] H. Bei, E.P. George, Acta Mater. 53 (2005) 69–77.